Received: 17 January 2022 | Revised: 28 March 2022 | Accepted: 29 March 2022

DOI: 10.1111/joa.13667

Journal of Anatomy ANATOMICAL SOCIETY WILEY

ORIGINAL ARTICLE

Structural abnormalities of retinal pigment epithelial cells in a light-inducible, rhodopsin mutant mouse

Debora Napoli[1,2] | **Enrica Strettoi**[1]

[1]Neuroscience Institute, Italian National Research Council, CNR, Pisa, Italy

[2]Regional Doctorate School of Neuroscience, University of Florence, Florence, Italy

Correspondence
Debora Napoli, Istituto di Neuroscienze Area della Ricerca, via Giuseppe, Moruzzi 1, 56124 Pisa, Italy.
Email: debora.napoli@in.cnr.it

Funding information
This research was funded by the Velux Foundation, Zurich (CH), project number 1236, and within a collaborative study under the frame of ERA-NET NEURON (NEURON-066 Rethealthsi).

Abstract

Retinal pigment epithelium (RPE) is a specialized pigmented monolayer dedicated to retinal support and protection. Given the fact that photoreceptor outer segments are the primary energy resource of RPE metabolism, it follows that, when photoreceptor function is compromised, RPE cells are impaired and vice versa. In retinitis pigmentosa (RP), genetic mutations lead to a massive degeneration of photoreceptors but only few studies have addressed systematically the consequences of rod and cone death on RPE cells, which, among others, undergo an abnormal organization of tight junctions (TJs) and a compromised barrier function. The biological mechanisms driving these barrier reorganizations are largely unknown. Studies aimed at addressing general and mutation-independent changes of the RPE in RP are relevant to reveal new pathogenic mechanisms of this heterogeneous family of diseases and prospectively develop effective therapeutic strategies. Here, we take advantage of a mouse model of RP in which retinal degeneration is spatially restricted to investigate a possible involvement of inflammatory responses in RPE remodeling. By immunostaining for Zona Occludens-1 (ZO-1), a structural and functional marker of TJs with pleiotropic functions, we found a partial rescue of TJs organization following local restoration of retinal organization, revealing that TJs structure can recover. Since lack of ZO-1 from TJs can alter cell density, we counted RPE cells without finding any differences between degenerated and controls animals, indicating preservation of RPE cells. However, we found an increased number of immune cells adhering to the RPE apical surface and a spatial correlation with areas of abnormal ZO-1 distribution. This suggests that inflammatory processes following photoreceptor degeneration can be responsible for TJs alterations during RP progression and deserve further investigation.

KEYWORDS
electron microscopy, inflammation, retinitis pigmentosa, retinal pigment epithelium, tvrm4, vacuoles

1 | INTRODUCTION

The retinal pigment epithelium (RPE) is a cuboidal monolayer located between the photoreceptors and the Bruch's membrane, a pentalaminar structure which separates RPE cells from the underlying fenestrate choroidal capillaries (Fuhrmann et al., 2014; Lakkaraju et al., 2020; Strauss, 2005). As all epithelia, the RPE shows an apical to basolateral polarity, which implicates a correspondingly uneven distribution of organelles and membrane proteins. The basolateral side is highly enfolded and selectively takes up nutrients (i.e., glucose, fatty acid, retinol, etc.) from the blood flow; nutrients are then delivered to the photoreceptors from the RPE apical side, which contains long, sheet-like microvilli. Metabolic wastes follow the opposite pathway (Bonilha et al., 2006; Yang et al., 2021). Given the fact that blood vessels dedicated to the outer retina are limited to the outer plexiform layer, the RPE represents an important source of metabolic support for photoreceptors (Sinha et al., 2020; Viegas & Neuhauss, 2021). This layer performs numerous additional functions: it actively participates to the visual circle by re-isomerization of all-trans-retinal to 11-cis-retinal; it maintains the ionic composition of the subretinal space guaranteeing the excitability of the photoreceptors; RPE cells phagocyte photoreceptor shed outer segments, ensuring a constant renewal of the photoreceptors tips (Kevany & Palczewski, 2010; Know and Freeman, 2020). The pigmented components of the RPE, represented by melanin and lipofucsin granules, absorb excess photons and protect the retina against photoxidation. Tight junctional (TJ) complexes among neighbors RPE cells contribute to maintain epithelial polarity, preventing the free diffusion of membrane proteins between apical and basolateral sides. More importantly, junctional complexes composed by occludins and claudins constitute a barrier preventing free diffusion from the choroidal space to the retina and back (Ivanova et al., 2019; Runkle & Antonetti, 2011). The TJ complexes confer a paracellular resistance 10 times higher than the transcellular one, so that the RPE is classified as a tight epithelium (Campbell & Humphries, 2012; Naylor et al., 2019). Finally, the RPE produces a plethora of soluble factors, such as growth factors and immunomodulators, which reach the retina and modulate its biology (Ming et al., 2009; Simó et al., 2010; Taylor et al., 2021; Taylor & Ng, 2018). It is known that the eye is endowed with immune privilege and the RPE participates in the establishment of this property. The RPE cells express on their surface membrane proteins able to induce apoptosis of immune cells, therefore modulating the eye immune response. Altogether, the number and variety of RPE functions make this layer and its proper functioning instrumental to ensure a proper retinal physiology.

The organization of the RPE might become affected in several pathological conditions (Sparrow et al.,2010), including retinitis pigmentosa (RP), a group of hereditary and heterogeneous retinal dystrophies clinically characterized by an early impairment of night vision followed by gradual visual field constriction until near blindness. Clinical symptoms reflect the degeneration patterns of photoreceptors: rods, responsible for night vision, degenerate first because typically genetic mutations affect rod-specific genes; cones, necessary for color vision and photopic acuity, follow later. The (still poorly understood) biological causes of cone secondary degeneration are an active research topic for the relevance that cones bear for human vision (Campochiaro & Mir, 2018; Guadagni et al., 2015; Narayan et al., 2016; Newton & Megaw, 2020; O'Neal & Luther, 2021). Downstream the genetic defect, multiple biological mechanisms contribute to the pathogenetic progression of RP. Recently, various studies pointed out that inflammatory responses triggered by dying rods become progressively exacerbated and significantly contribute to the disease progression (Campochiaro & Mir, 2018; Guadagni et al., 2015; Narayan et al., 2016; Newton & Megaw, 2020); Guadagni et al., 2019; Kaur & Singh, 2021). The first evidence of the inflammation involvement was obtained from anatomical observations of post-mortem retinas of RP patients, which showed altered number and morphology of the resident immune cells (microglia) (Gupta et al., 2003; Indaram et al., 2015). Similar changes have been documented in RP mouse models as well, where time-lapse imaging of retinal explant demonstrated that the phagocytic activity of the activated microglia extends also to intact (i.e., not dying) photoreceptors (Roque et al., 1996; Thanos et al., 1992). Finally, different pharmacological and genetic manipulations of microglia demonstrate that perturbations of the inflammatory/immune responses could rescue cones and have beneficial effects on visual function (Kaur & Singh, 2021; Ortega & Jastrzebska, 2021).

Given the proximity and metabolic relations with photoreceptors, it is likely that inflammatory responses triggered by RP also contribute to abnormalities found in the RPE in this disease. Several studies have demonstrated that immune cells release metalloproteases which are able to induce degradation of junctional complexes, in particular, digestion ofthe protein Zonula occludens 1 (ZO-1), causing outer barrier dysfunction, or releasing cytokines which can modulate the expression of TJ proteins (Gawdi & Emmady, 2020; Giebel et al., 2005; Jo et al., 2019; Kim et al., 2020; Matsubara et al., 2020; Zhou et al., 2010).

In a previous study, we demonstrated that structural RPE alterations occur in three different RP mouse models, where ZO-1 distribution in the RPE becomes discontinuous and the barrier properties of RPE impaired. Tight junction integrity can be rescued by Dexamethasone, used to effectively target retinal inflammation (Napoli et al., 2021). Here, we use a light-inducible model of RP, the Rho^{Tvrm4} ("Tvrm4") mouse, which exhibits a peculiar isolation of the photoreceptor degenerating area compared to the intact one. Several morphological parameters of RPE cell organization suggest that, in this mutant, the RPE becomes abnormal, without evidence of cell loss. We show that a correlation exists between discontinuities in ZO-1 distribution and areas of immune cells accumulation in the subretinal space, suggesting a possible source of RPE barrier alterations.

2 | METHODS

2.1 | Animal procedures

Mice used in all the experiments were of the strain. All animals originally came from Jackson Laboratory. Then, they were housed in standard cages with food and water ad libitum under a 12-h

light–dark cycle. Temperature and illumination were constantly monitored in order to be maintained at 22°C with an average illumination level of 1.2 cd/m^2. All experiments were carried out in accordance with the current regulations as reported in the Institutional Review Board Statement. All tissue explants were performed at the same time of the day (11–13 am) and a minimum of $n = 3$ animals were used per experimental group.

2.2 | Mice

Heterozygous (HT) Tvrm4 mice (RhoTvrm4/Rho+) on a C57Bl6J background were characterized by PCR genotyping and grew up to the age of 2–3 months. Animals for experiments were divided into control and induced mouse groups. The induced mice were dark adapted for 4 hrs in a black cage and then treated with eye drops to dilate the pupil (1 µl of 0.5% atropine, Allergan) (Gargini et al., 2017). After 10 min, mice were placed in a black illumination chamber described before [18] to be exposed for 2 min to a 12,000 Lux intensity (Philips Master TL5 HE 28 W/840, length 115 cm; 104 lm/W cool white mercury lamps). Mice were then returned to their cages, in normal animal house illumination conditions and harvested 1 months post induction (PI) to obtain ocular samples. A total of 12 Tvrm4 mice were used.

2.3 | RPE and retinal preparation

Mice were anesthetized by intraperitoneal injections of Zoletil 100 (80 mg/kg); their eyes were enucleated and marked for orientation on the dorsal periphery while mice were then quickly sacrificed. Eyes were first engraved at the level of the anterior chamber and submerged in 4% formaldehyde for 30 min at room temperature. Then, the anterior segment was removed and the eyecups were fixed again in 4% formaldehyde for other 30 min at room temperature. Finally, the eyecups were washed with tampon phosphate (0.1 M, pH = 7.4) and cryoprotected in 30% sucrose solution for one night at 4° C before were embedded in Tissue-Tek O.C.T. compound (4583, Sakura Olympus, Italy) on dry ice and stored at −20 °C until they were used. To start with immunocytochemistry (ICCH) protocol, eyes were cut toward the optic nerve head and the retina was gently separated from sclera/choroid RPE and the two were processed independently. The sclera-choroid and RPE were further cut radially with additional 4 to 8 incisions. First, the samples were incubated O/N at 4°C in a blocking PBS solution with 5% serum and 0.3% Triton-X 100, then they were incubated with primary antibodies solution (1% serum and 0.1% Triton-X 100 in PBS) against ZO-1 (rat polyclonal, MABT11; Merck-KGaA) and Iba1 (rabbit polyclonal; FUJIFILM Wako Chemicals U.S.A. Corp.) both diluted 1:400, for 3 days, at 4 °C. After washing for 30 min with PBS, the RPE samples were incubated for 2 h at room temperature in a secondary antibodies solution with 1% serum and 0.1% Triton-X 100 in PBS (anti-rat IgG, conjugated with Alexa Fluor 488 and anti-rabbit IgG, conjugated with Alexa Fluor 568, all from Invitrogen, Termofisher Scientific). Finally, the samples were counterstained with Hoechst (0.02 mg/ml) for 1 h and washed for 30 min in PSB. In parallel retinal samples were stained with an antibody against Cone Arrestin diluted 1:1000 (rabbit polyclonal, AB15282, Merck-KGaA). Then, the samples were flat mounted on glass slides and covered with Vectashield antifade mounting medium (Vector).

2.4 | Imaging

RPE flatmounts were imaged with a Zeiss Imager.Z2 microscope equipped with an Apotome2 device (Zeiss), using a Plan Neofluar 40X,

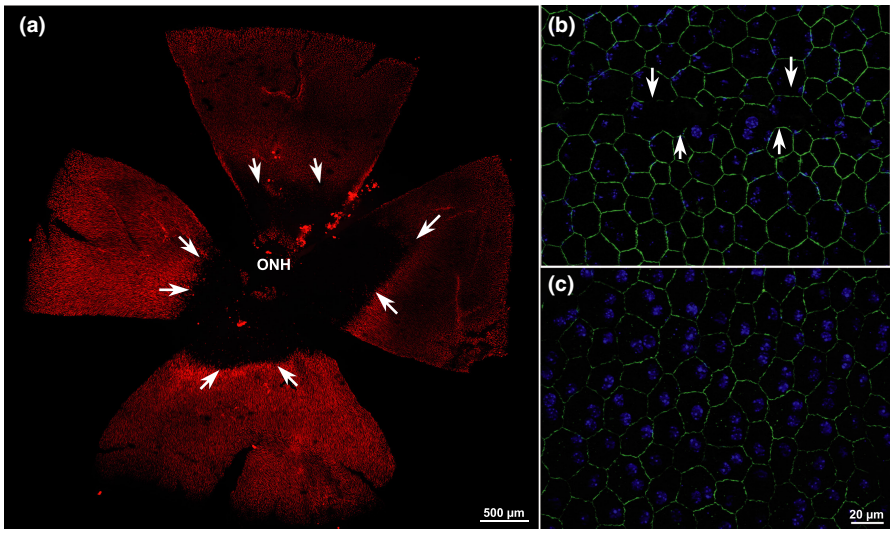

FIGURE 1 RPE has TJs alterations during retinal degeneration. (a) Whole-mount image of a TVRM4 retina 1 month post light-induction. Immunostaining for cone arrestin (red signal) highlights how the central retinal area is totally devoid of fluorescence, as most cones have degenerated (arrows). ONH: Optic nerve head. ZO-1 staining (green signal) of whole mount RPE from central, induced ocular area (b) and from an intact, peripheral region (c). Blue signal: Nuclear counter staining. Arrows in b indicate interruptions of ZO-1 positive profiles

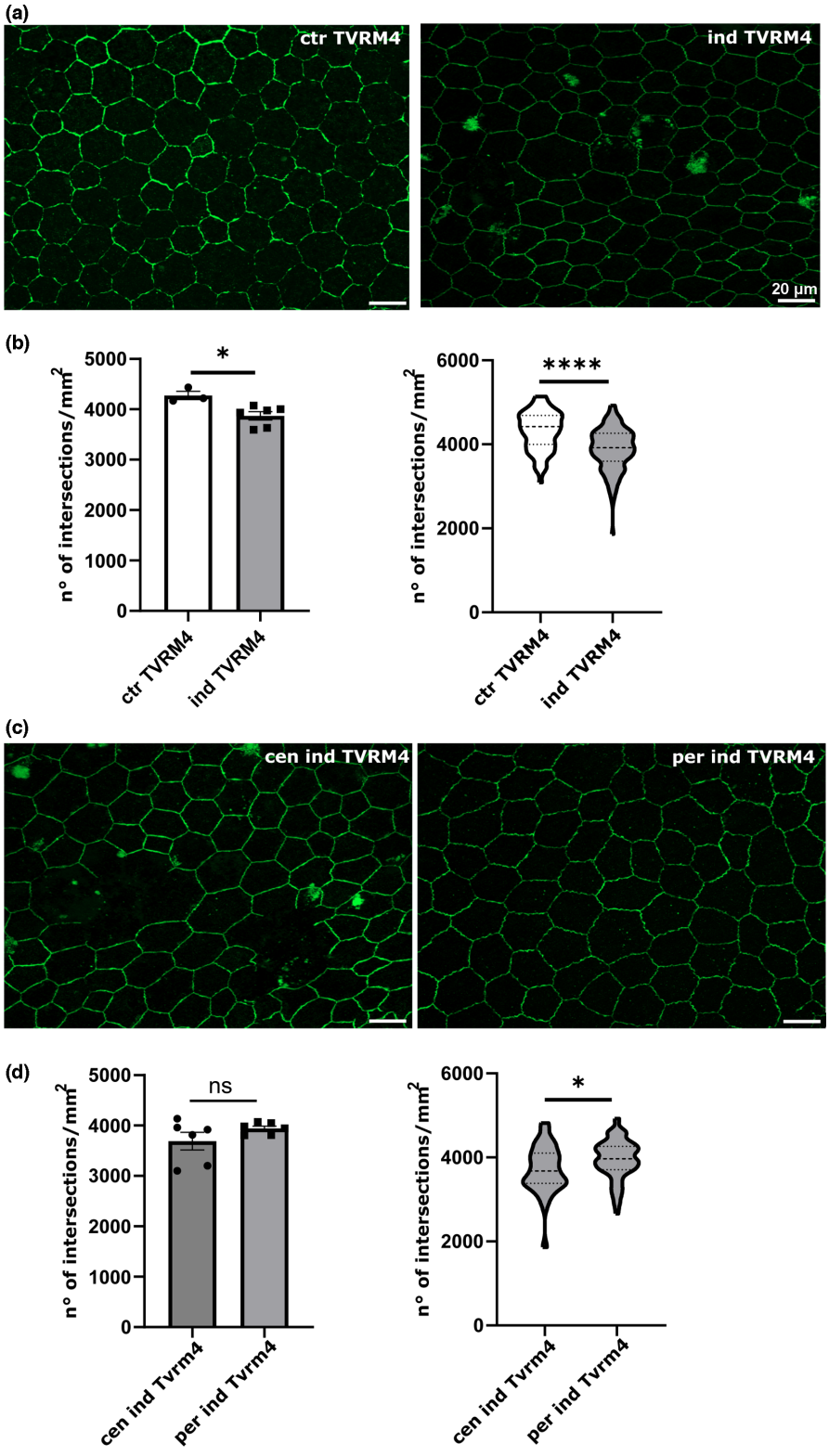

FIGURE 2 TJs is altered in induced TVRM4 respect to control animals but (a) Flatmounts of RPE from TVMR4 mice, 1 month post light-induction. ZO-1 immunostaining (green signal). Representative images of control animals (ctr TVRM4, left) and of induced mice (ind TVRM4, right). (b) Quantification of ZO-1 distribution. Comparison between control ($n = 3$) and induced mice ($n = 6$). Left, unpaired t-test, $p = 0.0184$. Right, violin plot of data distribution. Error bars represent ±SEM. $^{*}p < 0.05$, $^{****}p < 0.0001$. (c) Flatmounts of RPE, ZO-1 immunostaining, ligh-induced TVMR4 mice. Representative images of central (cen, ind TVRM4, left) and peripheral areas (per, ind TVRM4, right). (d) Quantification of ZO-1 distribution and comparison between central (cen ind TVRM4, $n = 6$) and peripheral areas (per ind TVRM4, $n = 6$). Paired t-test, $p = 0.1193$. Error bars represent ±SEM. Ns, not significant differences

1.25 oil objective. ZO-1-stained samples were acquired regularly along 4 radial axes; optimally flattened areas were chosen and images from 1–2 central and 4 mid-peripheral with respect to the optic nerve zones were done, for a total of 16–20 sampling-fields measuring (224 × 168) μm. Each final image was generated as a projection of z-stacks acquisitions by Zeiss software ZEN®2, which was also used to adjust brightness and contrast of the pictures. Finally, Image J was used to count RPE cells, nuclei, and quantify ZO-1 profile. To achieve this last point a custom grid (with 20 μm-spaced mashes) was generated and overlapped to ZO-1 images profiling to count the number of the intersection points between the two images. Tiled images of RPEs and corresponding retinal leaflets were also obtained at low magnification and stored. Image J data were collected in an excel file and statistically analyzed with GraphPad 8.0.2.

2.5 | Electron microscopy

Tvrm4 mice were light-induced and retinal preparations were done as also previously described. In summary, eye cups were fixed in 1% glutaraldehyde-2% vol/vol PFA in Sorenson's buffer M/30 (pH 7.4 + 5% wt/vol sucrose) for 2 h at 4 °C, dissected in quadrants and postfixed in 3% for 12 h, at 4°C. Tissue blocks were infiltrated with 3% potassium ferrocyanide +2% OsO4 in H2O, at 4°C; bloc stained with 1% uranyl acetate (in 0.05 M maleate buffer, pH 6), then dehydrated with a series of ethanol and flat embedded in Epon/Araldite. Ultrathin sections, 90 nm thick, were obtained from the central retinas of light-induced and control samples, collected on single hole, formvar-coated grids, and observed with a Jeol 1200EXII electron microscope. Images were obtained at various magnifications with a Gatan high-resolution cooled camera.

2.6 | Statistical analysis

All data were analyzed using GraphPad Prism 8.0.2. The value of each image counting was reported in an excel file and used to calculate the mean or normalized to mm^2. GraphPad was used for the final statistical analysis. Data were shown as mean ± standard error of mean (SEM), where each mean is obtained from 1 mouse or as distribution of all images counting. Statistical comparisons were conducted by means of two-tailed, unpaired, or paired Student's *t*-test. Correlations were calculated using linear regression and Pearson coefficient.

3 | RESULTS

3.1 | RPE organization of TJs shows some rescue

TJs are multiprotein complexes of cell-to-cell contacts with the essential function to control the paracellular diffusion between different compartments ensuring the maintenance of tissue homeostasis. Typically, epithelial and endothelial cells with barrier properties express tight junctional proteins at their apical side, including RPE cells forming the outer retinal barrier. ZO-1 is a scaffold protein of TJs, generally used as a marker of structural and functional integrity of these complexes. In some retinal degeneration conditions such as diabetic retinopathy and macular degeneration, leakage of the outer retinal barrier is a pathogenic process. In these cases, ZO-1 profile among RPE cells is altered. In a previous analysis, we examined RPE integrity in three different mouse models of RP using ZO-1 immunostaining, which demonstrated evident discontinuities, corresponding to areas of barrier leakage, as assessed by intravenous injections of fluorescent tracers. Among the mouse models, we also used TVRM4 mice, whose retina degenerates after a strong light induction following a central-peripheral pattern. RPE TJs alterations follow the same pattern suggesting that they are affected by retinal damage (Napoli et al., 2021). Based on the previous finding that 1 month after light-induction TVRM4 animals show a partial rescue of the central retina morphology and function (Gargini et al., 2017), we asked whether also the RPE showed a remodeling attenuation (Figure 1a–c). Thus, we investigated ZO-1 density in the RPE of TVRM4 mice 1 month after light induction using the same methodological approach used before. We overlapped a custom-grid to images of ZO-1 staining and counted the intersections points. As expected, we found a significant difference of ZO-1 staining between induced TVRM4 mice and age-control animals (Figure 2a,b). However, we did not find the large difference in ZO-1 distribution between central and peripheral areas (Figure 2c,d) observed 1-week post-induction, as the decreased density of ZO-1 processes in the central part of the RPE was attenuated. This shows that the integrity of the TJs was partially restored.

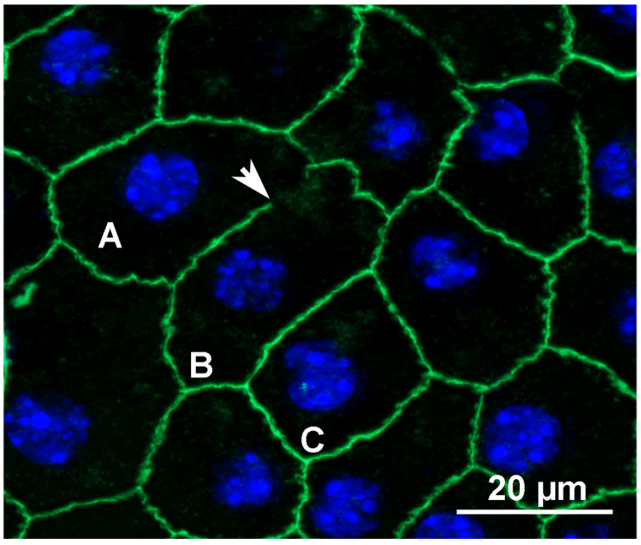

FIGURE 3 ZO-1 do not translocate to the nucleus. This image shows the lack of ZO-1 staining (green signal) into nuclei (blue signal) of in both cells with normal (C) and impaired TJs (A,B). Arrow shows ZO-1 interruption

3.2 | Lack of ZO-1 induces neither density changes nor multinucleation

Knowing that loss of epithelial markers such as ZO-1, in parallel with inflammatory exposure, can induce an epithelial-mesenchymal transition and that ZO-1 itself can translocate into the nucleus to regulate cell proliferation, we investigated RPE cell density in induced and age-matched control animals (Neyrinck-Leglantier et al., 2021; Zhou et al., 2020; Chen et al., 2016). We first asked whether ZO-1 translocated in the nucleus of RPE cells upon light induction. No colocalization of nuclear staining and ZO-1 signal was detected in control (non-induced) as well as in light-induced animals; lack of nuclear translocation was evident both for normal cells and damaged RPE (Figure 3). In agreement with these results, we found that the overall RPE cell density in induced mice was very close to that of controls (Figure 4a). However, RPE cells of induced animals differed from control mice in their shape (Figure 4c,d), which appeared evidently more irregular, preferentially rounded, or elongated and spindle-shaped, rather than classically hexagonal. To gain indications about RPE cell viability, we counted multinucleate cells in induced and control mice, insofar RPE cells are considered differentiated, post-mitotic cells and become multinucleated under stress conditions. Again we did not find any difference between induced and control groups (Figure 4b), suggesting that the main remodeling is confined to barrier alterations.

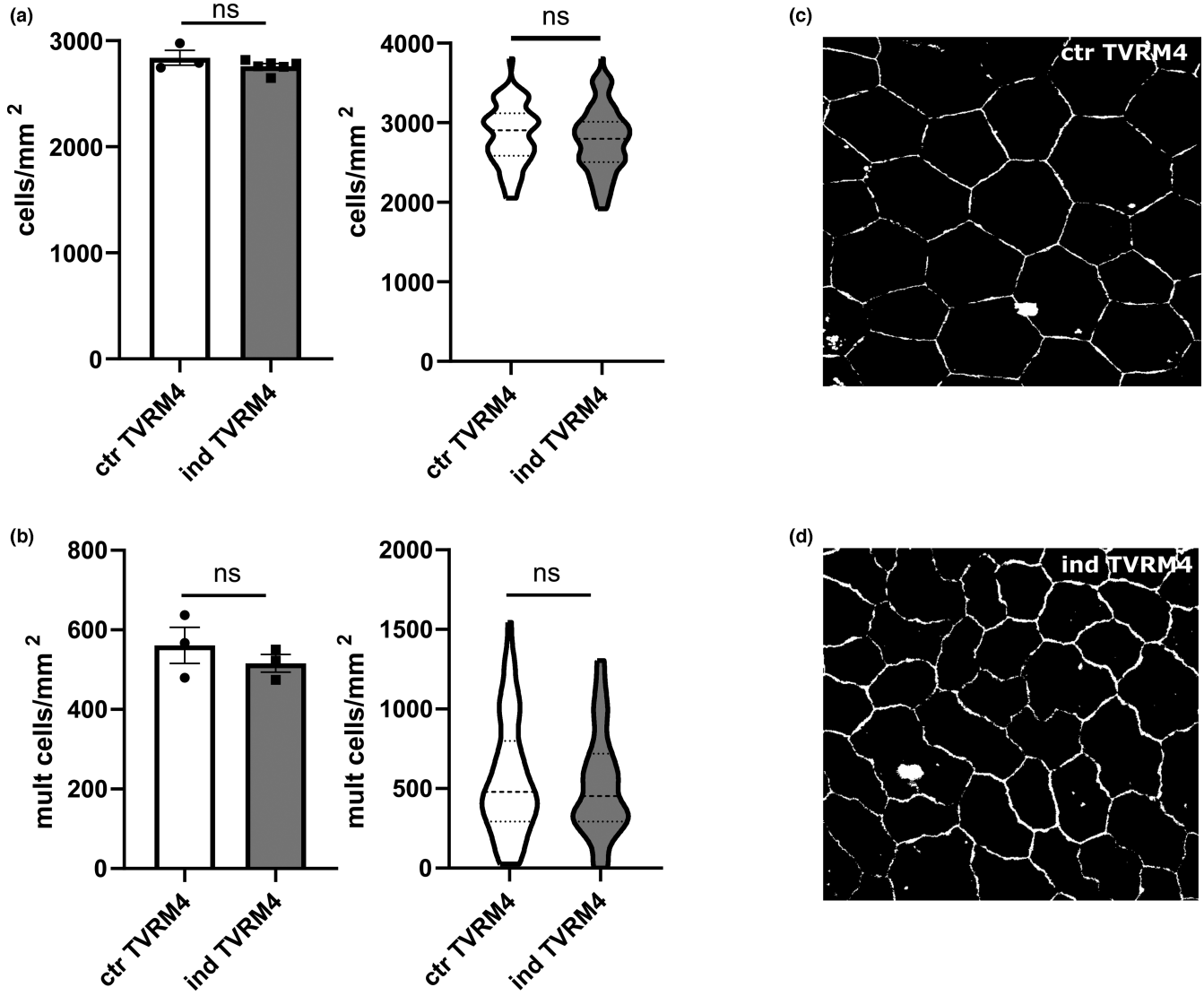

FIGURE 4 RPE cells of induced TVRM4 have altered shape but no changes in density or nuclei distribution. (a) Comparison of RPE cell density between controls (ctr TVRM4, $n = 3$) and induced TVRM4 mice (ind TVRM4, $n = 6$). Unpaired t test (left), $p = 0.217$; violin plot showing data distribution (right), $p = 0.2678$ (b). Comparison of multinucleate cell density between controls (ctr TVRM4, $n = 3$) and induced TVRM4 mice (ind TVRM4, $n = 3$). Unpaired t test (left), $p = 0.4226$; violin plot showing data distribution (right), $p = 0.4603$ (c) binary images representing different shapes of RPE cells in (c) controls (ctr TVRM4) and (d) induced TVRM4 (ind TVRM4) mice

3.3 | RPE vacuolization and apical microvilli elongation

To deepen the analysis of RPE cells during retinal degeneration, we carried on initial electron microscopy observations on retinal samples of induced mice, comparing centrally induced and peripheral (intact) areas. We confirmed the presence of an abundant collection of small and very large vacuoles in the cytoplasm of RPE cells of the central area. These vacuoles had no ultrastructural details and appeared electron-lucent and were concentrated toward Bruch's membrane. Numerous melanin granules of different sizes were also evident and disorganized apical microvilli abutting the degenerated outer segment layer. It is known that experimental downregulation of ZO-1 expression in RPE induces vacuolization of pigmented cells (Georgiadis et al., 2010). Our observation can therefore describe the generalized effects of ZO-1 decrement and reorganization on the hydrolytic balance of this layer.

3.4 | Accumulation of Iba+cells correlated with ZO-1 discontinuities

Microscopy observations of RPE flatmounts revealed an accumulation of autofluorescent aggregates on RPE cells of induced TVRM4 mice similar to those described in the past (Figure 6a,b; (Aredo et al., 2015; Zhang et al., 2019). Thus, we asked whether these aggregates had an immune system origin, since it is known that invasion of the photoreceptor layer and subretinal space by immune cells occurs in RP, at the times when the inflammatory response by resident microglia and infiltrating monocytes is initiated. To investigate the identity of autofluorescent cells juxtaposed to the apical face of the RPE, we performed an immunostaining against Iba-1 (Ionized calcium-binding adaptor molecule 1), a microglial and macrophage-specific calcium-binding protein widely used as marker of immune cells. Most cells were positive for Iba-1 staining (Figure 7a–d) as expected, but not all of them, suggesting that other phagocytic cells could reach the subretinal space. Moreover, Iba1+ cells had different morphologies (i.e., typically ramified or ameboid) (Figure 5c,d), suggesting differences in their function (Rashid et al., 2019; Rathnasamy et al., 2018; Silverman & Wong, 2018). Counting of the Iba1+ cells on RPE flatmounts revealed a significant increase in Tvrm4 light-induced mice with respect to age-matched controls, and a significantly different distribution between central and peripheral areas of induced mice, with higher density of Iba+cells located in central regions (Figure 8a,b). To study the topographical relation of RPE discontinuities and immune system cells, we took advantage of the relative isolation of the degenerating ocular area, well separated from the intact portions. We carried on a statistical correlation analysis between ZO-1 profiling and the number of Iba-1+ cells counted in the same region, analyzing induced and non-induced TVRM4 cases (Figure 8c) and data from induced mice alone (Figure 8d). We found a significantly negative correlation between these two variables, insofar the number of Iba1+ cells correlated with the occurrence of ZO-1 discontinuities in the RPE. The result obtained does not take into consideration the heterogeneity of the Iba-1+ cells counted.

4 | DISCUSSION

RP is a genetic retinal disease that strongly affects photoreceptor survival leading to blindness. Given the large heterogeneity of the causative mutations, the possibilities to develop a general-use gene therapy are currently low; hence, studying the mechanisms that contribute to the pathogenesis of RP is fundamental for developing

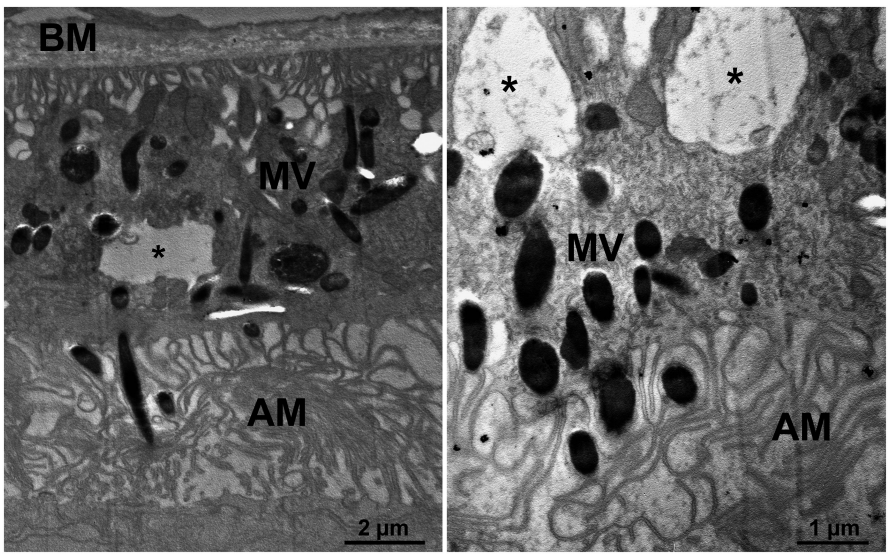

FIGURE 5 RPE cells of induced mice contain vacuoles with different sizes. Electromicrographs of RPE sections. TVRM4 mouse, light-induced area. Both small and vary large vacuoles (asterisks) with apparent lack of ultrastructure fill RPE cells mostly concentrated in the proximity of Bruch's membrane (BM). Apical microvilli (AM) appear long and irregular. MV, Melanin vesicles

mutation-independent therapeutic strategies. The RPE is strictly related to photoreceptors from a functional and structural point of view and yet little is known about the consequences of massive photoreceptor death on RPE function in RP. In a previous work we described that photoreceptor degeneration is accompanied by structural alterations of TJs and functional impairment of the RPE barrier properties in three different mouse models of RP (Napoli et al., 2021). This dysfunctionality can heavily contribute to the pathogenetic progression of the disease. Without a proper barrier protection, the outer retina becomes more exposed to external and internal injuries (including the infiltration of circulating macrophages), which can contribute to worsening the pathology. However, the mechanisms underlying RPE dysfunction in RP have not been investigated systematically. Understanding the biological processes responsible for TJs and RPE cell dysfunctions in RP may offer new targets to protect photoreceptors and slow down their degeneration in this disease.

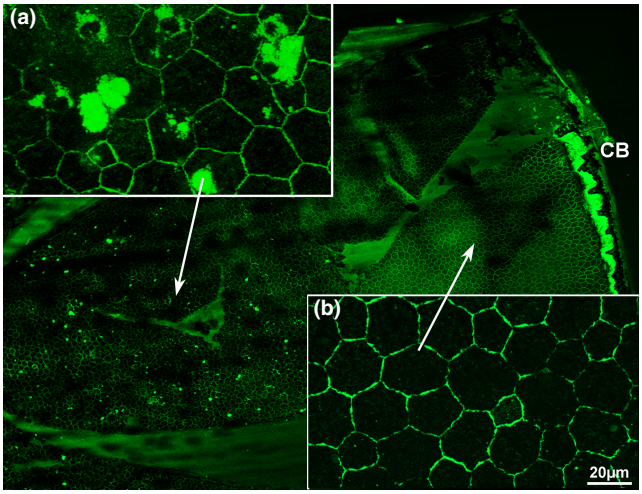

FIGURE 6 Accumulation of autofluorescent aggregates on the apical face of induced RPE. The central part of the image is occupied by a large leaflet of RPE from TVRM4 mouse, 1 month after light induction, stained for ZO-1 (green signal). The central retina is on the left and the periphery on the right. CB, Ciliary body. (a) and (b) are higher magnification of central and peripheral regions respectively. Clustering of autofluorescent bodies is evident in (a)

Here, we begin to investigate possible processes responsible for RPE dysfunction, taking advantage of a peculiar mouse model (the TVMR4), which shows a spatially confined retinal degeneration and which undergoes a partial reversion of the retinal phenotype 1 month after light-induction (Gargini et al., 2017; Stefanov et al., 2020).

First, we demonstrate that the known rescue of retinal organization is accompanied by TJ morphological recovery in the RPE, suggesting that TJs have been not irreversibly compromised and can spontaneously recover the physiological structure.

We studied the TJ organization by assessing the distribution of ZO-1, a structural and functional regulator of junctional complexes, being equipped with different protein domains for interacting with several other proteins. At junctional plaques, ZO-1 is indispensable for claudin polymerization at TJs pores and connection with perijunctional actomyosin ring, necessary for the junctional tone Brunner et al., (2021). ZO-1 is also involved in signal transduction and transcriptional modulation that primarily culminate in the control of cell density and proliferation. Nuclear localization (NLS) and nuclear export signals (NES) enable ZO-1 to shuttle between the cytoplasm and the nucleus to control the remodeling of cell–cell contacts, although it is not clear which genes are controlled (Gottardi et al. 1996). ZO-1

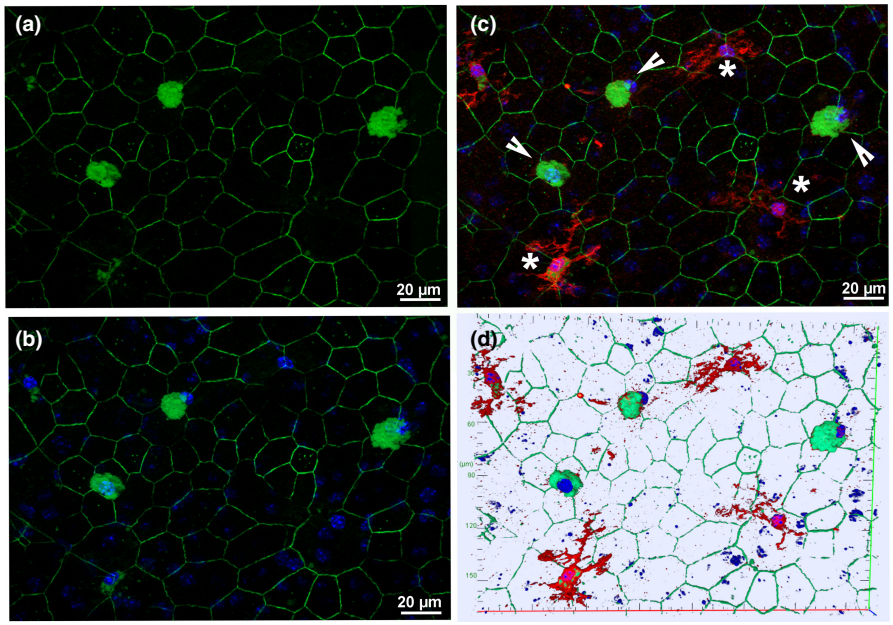

FIGURE 7 Aggregates are iba+ positive cells. Flatmounts of RPE, Iba1 immunostaining. Representative image of (a) autofluorescent aggregates, (b) Hoechst nuclear staining with ZO-1(green signal) and (c) Iba1+ cells (red signal) overlying the RPE; (d) digital representation of c. arrows: Ameboid cells. Asterisks: Ramified cells

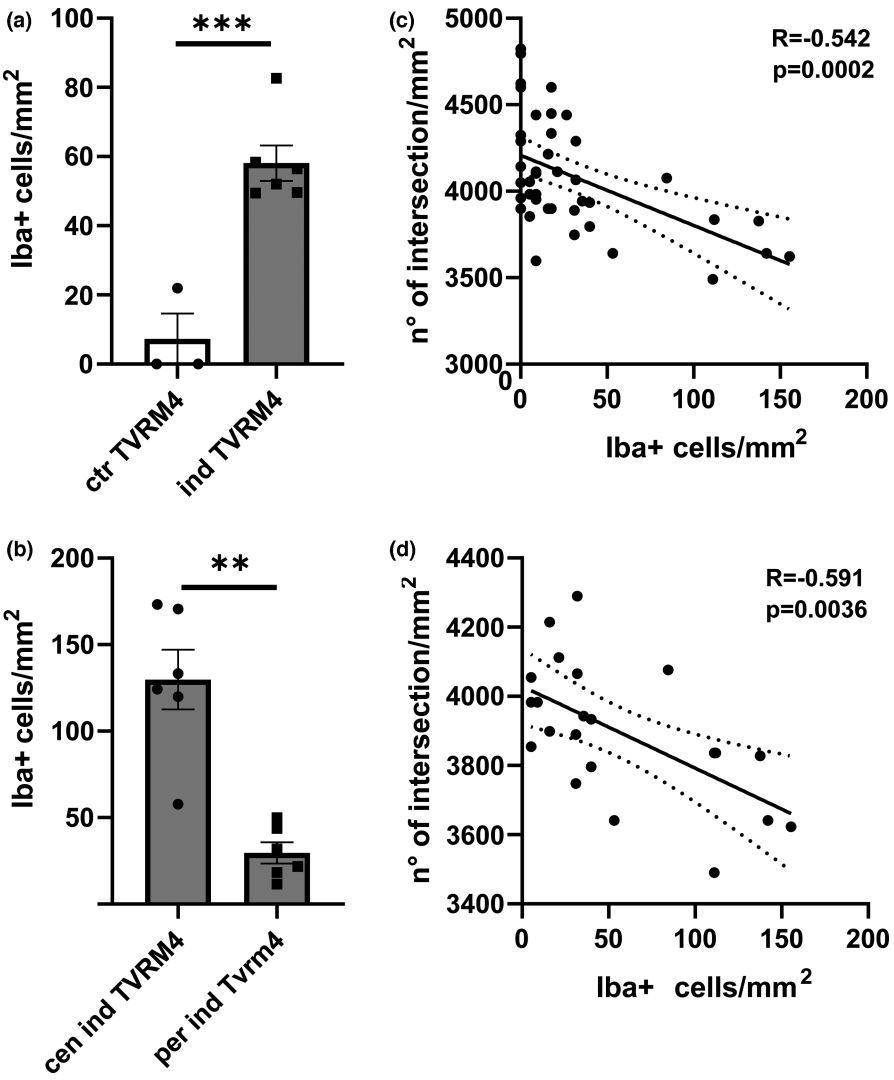

FIGURE 8 Distribution of Iba+cells on RPE and altered ZO-1 profile are correlated. ZO-1 interruptions and accumulation of Iba+cells are quantification of iba1+ cells density and comparison between control (ctr TVRM4, $n = 3$) and induced mice (ind TVRM4, $n = 6$). (a) Unpaired t test, $p = 0.0007$. Right, violin plot showing data distribution. (b) Comparison between central (cen ind TVRM4, $n = 6$) and peripheral areas (per ind TVRM4, $n = 6$). Paired t test, $p = 0.0049$. Right, violin plot showing data distribution. Error bars represent ±SEM. ***$p < 0.05$, ****$p < 0.0001$. (c) Scatter plot showing correlation between Iba1+ cells density and lack of ZO-1 staining assessed on RPE flatmounts. (c) Analysis performed including data from all controls and induced TVRM4 cases. Pearson correlation: $R = -0.514$, $p = 0.0002$. (d) Analysis performed including only data of induced TVRM4. Pearson correlation: $R = -0.593$, $p = 0.0036$

can also regulate the nuclear translocation of transcription factors such as ZONAB and alpha-catenin (Georgiadis et al., 2010; Chai et al. 2010). In normal TJ organization, these factors are kidnapped to the junctional complexes through ZO-1. When ZO-1 is absent from TJs, they move to the nucleus to control proliferation and cell density genes (Balda et al. 2003). In our samples, although ZO-1 continuity is interrupted in TJs from degenerating areas, no localization into the nucleus nor change in RPE cell density were observed, suggesting that the main consequence of the lack of ZO-1 from TJs is mainly a dysfunction of the outer blood-retinal barrier. Despite the potential toxic environment created by retinal degeneration, the overall viability of RPE cells seems to be normal, as suggested by the fact that the number of multinucleated cells is similar in control and induced mice. Multinucleation of RPE cells is mostly documented in aging and pathological conditions (i.e., age-related macular degeneration, AMD) and is considered a cellular strategy to overcome stress injuries (Chen et al., 2016; Rajapakse et al., 2015). When an RPE cell dies, it may secrete signals to neighboring cells to enlarge their size and replicate the genetic material. This would ensure the continuity of the monolayer function. Albeit not multinucleated, RPE cells of TVRM4 mice appear more irregular in the areas exposed to light-induction and, because of TJ breakdown, they have likely lost their cellular tone, normally maintained by a coupling of the cytoskeleton with TJs cellular membrane.

TJ alterations together with cytoskeleton reorganization may be the consequences of a physiological process in which the RPE

actively participates allowing the entry of circulating macrophages from the choroidal plexus to the degenerated retina. Activated immune cells (i.e., resident microglia and infiltrating macrophages) release metalloproteases and cytokines that, respectively, directly and indirectly, can regulate ZO-1 expression (Byrne et al., 2021; Capaldo & Nusrat, 2009; Huang et al., 2020; Jo et al., 2019). Indeed, we found a significant correlation between the areas enriched with Iba + cells and the areas where ZO-1 is missing. In normal condition, RPE cells express on the surface ligands (i.e., Fas-ligand) and secrete immunomodulators as transforming growth factor-beta2 and alpha-melanocyte stimulating factor to prevent immune cells accumulation in the subcellular space (Taylor et al., 2021). It is possible that, in case of need, RPE cells stop producing these molecules to allow those neuroprotective immune cells that should enter the subretinal space. Indeed, single-cell RNA sequencing of immune cells of the subretinal space in a mouse model of RP revealed an enrichment of neuroprotective immune cells necessary for RPE preservation (O'Koren et al., 2019; Yu et al., 2020). Then, finally when photoreceptor degeneration goes down and inflammatory responses lower, RPE cells could repristinate their tight junction assessment. The scenario of inflammatory responses during this RP is evidently complex and requires further investigation.

Otherwise and/or in addition, the discontinuities in ZO-1 arrangement could represent a feature of stressed RPE cells. RPE metabolism is strictly dependent from fatty acid β-oxidation, in turn resulting from outer segment phagocytosis (Hurley, 2021; Sinha et al., 2020). Thus, when photoreceptors die, RPE cells lose a reservoir of energy. How this is related to a change in ZO-1 expression is not known. One possible explanation could be the activation of mTOR pathway, an evolutionary conserved signaling triggered by several stimuli including stress conditions. As previously demonstrated, a selective RPE oxidative phosphorylation impairment perturbs RPE morphology and junctional integrity which are preserved by rapamycin administration, a pharmacological inhibitor of mTOR pathway (Zhao et al., 2011).

Ultrastructural observations of induced TVRM4 mice confirmed alterations similar to those observed in models of macular degeneration and recently in rd1 mouse model of RP (Fujihara et al., 2008; Georgiadis et al., 2010; Saint-Geniez et al., 2009; Wu et al., 2021). The common presence of small and large vacuoles suggests an impairment of the ability of the RPE to control the electrolytic balance at the outer and inner membranes and suggests further analysis of biochemical pathways regulating this delicate process.

In conclusion, we first observed that RPE cells have TJs that break and can partially repair upon massive photoreceptor death. Loss of ZO-1 from TJs does not alter RPE cell density or induce multinucleation but abnormal, irregular morphology develops and vacuolization is detected ultrastructurally. Multiple ruptures in TJs correlate with the accumulation of immune cells in the subretinal space, suggesting that inflammatory responses may play a fundamental role in their development, reinforcing the need to study this process in inherited photoreceptor degenerations.

ACKNOWLEDGMENTS

The authors would like to thank the lab collaborators Noemi Orsini and Beatrice Di Marco for support through the study and Elena Novelli for tecnnical support. Open Access Funding provided by Consiglio Nazionale delle Ricerche within the CRUI-CARE Agreement.

DATA AVAILABILITY STATEMENT

Derived data supporting the findings of this study are available from the authors Debora Napoli and Enrica Strettoi on request.

ORCID

Debora Napoli https://orcid.org/0000-0003-1002-4244

REFERENCES

Aredo, B., Zhang, K., Chen, X., Wang, C.X.-Z., Li, T. & Ufret-Vincenty, R.L. (2015) Differences in the distribution, phenotype and gene expression of subretinal microglia/macrophages in C57BL/6N (Crb1 rd8/rd8) versus C57BL6/J (Crb1 Wt/wt) mice. *Journal of Neuroinflammation*, 12, 6.

Balda, M.S., Garrett, M.D. & Matter, K. (2003) The ZO-1-associated Y-box factor ZONAB regulates epithelial cell proliferation and cell density. *Journal of Cell Biology*, 160(3), 423–432.

Bonilha, V.L., Rayborn, M.E., Bhattacharya, S.K., Xiarong, G., Crabb, J.S., Crabb, J.W. et al. (2006) The retinal pigment epithelium apical microvilli and retinal function. In: *In retinal degenerative diseases, 519–24*. US: Springer.

Brunner, J., Ragupathy, S. & Borchard, G. (2021) Target specific tight junction modulators. *Advanced Drug Delivery Reviews*, 171, 266–288.

Byrne, E. M., Llorián-Salvador, M., Tang, M., Margariti, A., Chen, M., and Xu, H. 2021. IL-17A damages the blood–retinal barrier through activating the Janus kinase 1 pathway. *Biomedicine*, 9(7), 831.

Campbell, M. & Humphries, P. (2012) The blood-retina barrier: tight junctions and barrier modulation. *Advances in Experimental Medicine and Biology*, 763, 70–84.

Campochiaro, P.A. & Mir, T.A. (2018) The mechanism of cone cell death in retinitis pigmentosa. *Progress in Retinal and Eye Research*, 62, 24–37.

Capaldo, C.T. & Nusrat, A. (2009) Cytokine regulation of tight junctions. *Biochimica et Biophysica Acta*, 1788(4), 864–871.

Chai, K., Kitamura, K., McCann, A. & Wu, X.R. (2010) The epithelium—molecular landscaping for an interactive barrier. *Journal of Biomedicine and Biotechnology*, 2010, 870506.

Chen, M., Rajapakse, D., Fraczek, M., Luo, C., Forrester, J.V. & Heping, X. (2016) Retinal pigment epithelial cell multinucleation in the aging eye - a mechanism to repair damage and maintain homoeostasis. *Aging Cell*, 15(3), 436–445.

Fuhrmann, S., Zou, C. & Levine, E.M. (2014) Retinal pigment epithelium development, plasticity, and tissue homeostasis. *Experimental Eye Research*, 123, 141–150.

Fujihara, M., Nagai, N., Sussan, T.E., Biswal, S. & Handa, J.T. (2008) Chronic cigarette smoke causes oxidative damage and apoptosis to retinal pigmented epithelial cells in mice. *PLoS One*, 3(9), e3119.

Gargini, C., Novelli, E., Piano, I., Biagioni, M. and Strettoi, E. 2017. Pattern of retinal morphological and functional decay in a light-inducible, rhodopsin mutant mouse. *Scientific Reports*, 7(1), 5730.

Gawdi, R. & Emmady, P.D. (2020) Physiology, blood brain barrier. In: *StatPearls*. Treasure Island, FL: StatPearls Publishing.

Georgiadis, A., Tschernutter, M., Bainbridge, J.W., Balaggan, K.S., Mowat, F., West, E.L. et al. (2010) The tight junction associated Signalling proteins ZO-1 and ZONAB regulate retinal pigment epithelium homeostasis in mice. *PLoS One*, 5(12), e15730.

Giebel, S.J., Menicucci, G., McGuire, P.G. & Das, A. (2005) Matrix metalloproteinases in early diabetic retinopathy and their role in alteration

of the blood–retinal barrier. *Laboratory Investigation; a Journal of Technical Methods and Pathology*, 85(5), 597–607.

Gottardi, C.J., Arpin, M., Fanning, A.S. & Louvard, D. (1996) The junction-associated protein, zonula occludens-1, localizes to the nucleus before the maturation and during the remodeling of cell-cell contacts. *Proceedings of the National Academy of Sciences of the United States of America*, 93(20), 10779–10784.

Guadagni, V., Biagioni, M., Novelli, E., Aretini, P., Mazzanti, C.M. & Strettoi, E. (2019) Rescuing cones and daylight vision in retinitis pigmentosa mice. *FASEB Journal: Official Publication of the Federation of American Societies for Experimental Biology*, 33(9), 10177–10192.

Guadagni, V., Novelli, E., Piano, I., Gargini, C. & Strettoi, E. (2015) Pharmacological approaches to retinitis pigmentosa: a laboratory perspective. *Progress in Retinal and Eye Research*, 48, 62–81.

Gupta, N., Brown, K.E. & Milam, A.H. (2003) Activated microglia in human retinitis pigmentosa, late-onset retinal degeneration, and age-related macular degeneration. *Experimental Eye Research*, 76(4), 463–471.

Huang, Z.Q., Liu, J., Ong, H.H., Yuan, T., Zhou, X.M., Wang, J. et al. (2020) Interleukin-13 alters tight junction proteins expression thereby compromising barrier function and dampens rhinovirus induced immune responses in nasal epithelium. *Frontiers in Cell and Developmental Biology*, 8, 572749.

Hurley, J.B. (2021) Retina metabolism and metabolism in the pigmented epithelium: a busy intersection. *Annual Review of Vision Science*, 7, 665–692.

Indaram, M., Ma, W., Zhao, L., Fariss, R.N., Rodriguez, I.R. & Wong, W.T. (2015) 7-Ketocholesterol increases retinal microglial migration, activation, and Angiogenicity: a potential pathogenic mechanism underlying age-related macular degeneration. *Scientific Reports*, 5, 9144.

Ivanova, E., Alam N.M., Prusky G.T., and Sagdullaev B.T.. (2019). Blood-retina barrier failure and vision loss in Neuron-specific degeneration. *JCI Insight*, 4, e126747.

Jo, D.H., Yun, J.H., Cho, C.S., Kim, J.H., Kim, J.H. and Cho, C.H. 2019. Interaction between microglia and retinal pigment epithelial cells determines the integrity of outer blood-retinal barrier in diabetic retinopathy. *Glia*, 67(2), 321–331.

Kaur, G., and Singh N.K.. 2021. The role of inflammation in retinal neurodegeneration and degenerative diseases. *International Journal of Molecular Sciences*, 23(1), 386.

Kevany, B.M. & Palczewski, K. (2010) Phagocytosis of retinal rod and cone photoreceptors. *Physiology*, 25(1), 8–15.

Kim, D., Kang, M.-K. & Kang, Y.-H. (2020) Eucalyptol blocks diabetes-associated disruption of tight junction and blood retinal barrier in retinal pigment epithelial cells and diabetic eyes. *Current Developments in Nutrition*, 4(Supplement_2), 413–413.

Kwon, W. & Freeman, S.A. (2020) Phagocytosis by the retinal pigment epithelium: recognition, resolution, recycling.. *Frontiers in Immunology*, 11, 604205.

Lakkaraju, A., Umapathy, A., Tan, L.X., Daniele, L., Philp, N.J., Boesze-Battaglia, K. et al. (2020) The Cell Biology of the Retinal Pigment Epithelium. *Progress in Retinal and Eye Research*, 78, 100846.

Matsubara, J.A., Tian, Y., Cui, J.Z., Zeglinski, M.R., Hiroyasu, S., Turner, C.T. et al. (2020) Retinal distribution and extracellular activity of granzyme B: a serine protease that degrades retinal pigment epithelial tight junctions and extracellular matrix proteins. *Frontiers in Immunology*, 11, 574.

Ming, M., Li, X., Fan, X., Yang, D., Liang, L., Chen, S. et al. (2009) Retinal pigment epithelial cells secrete neurotrophic factors and synthesize dopamine: possible contribution to therapeutic effects of RPE cell transplantation in Parkinson's disease. *Journal of Translational Medicine*, 7, 53.

Napoli, D., Biagioni, M., Billeri, F., Di Marco, B., Orsini, N., Novelli, E. and Strettoi, E. 2021. Retinal pigment epithelium remodeling in mouse models of retinitis pigmentosa. *International Journal of Molecular Sciences*, 22(10), 5381.

Narayan, D.S., Wood, J.P., Chidlow, G. & Casson, R.J. (2016) A review of the mechanisms of cone degeneration in retinitis pigmentosa. *Acta Ophthalmologica*, 94(8), 748–754.

Naylor, A., Hopkins, A., Hudson, N. and Campbell, M. 2019. Tight junctions of the outer blood retina barrier. *International Journal of Molecular Sciences*, 21(1), 211.

Newton, F., and Megaw, R.. 2020. "Mechanisms of photoreceptor death in retinitis pigmentosa." *Genes*, 11(10), 1120.

Neyrinck-Leglantier, D., Lesage, J., Blacher, S., Bonnomet, A., Hunziker, W., Noël, A. et al. (2021) ZO-1 intracellular localization organizes immune response in non-small cell lung cancer. *Frontiers in Cell and Developmental Biology*, 9, 749364.

O'Koren, E.G., Yu, C., Klingeborn, M., Wong, A.Y., Prigge, C.L., Mathew, R. et al. (2019) Microglial function is distinct in different anatomical locations during retinal homeostasis and degeneration. *Immunity*, 50(3), 723–37.e7.

O'Neal, T.B. & Luther, E.E. (2021) Retinitis pigmentosa. In: *StatPearls*. Treasure Island (FL): StatPearls Publishing.

Ortega, J.T., and Jastrzebska, B.. 2021. Neuroinflammation as a therapeutic target in retinitis pigmentosa and quercetin as its potential modulator. *Pharmaceutics*, 13(11), 1935.

Rajapakse, D., Chen, M. & Heping, X. (2015) Photoreceptor outer segment (POS) suppresses RPE cell proliferation and induces multi-nucleation. *Investigative Ophthalmology & Visual Science*, 56(7), 2323–2323.

Rashid, K., Akhtar-Schaefer, I. & Langmann, T. (2019) Microglia in Retinal Degeneration. *Frontiers in Immunology*, 10, 1975.

Rathnasamy, G., Foulds, W.S., Ling, E.-A. & Kaur, C. (2018) Retinal microglia – a key player in healthy and diseased retina. *Progress in Neurobiology*, 173, 18–40.

Roque, R.S., Imperial, C.J. & Caldwell, R.B. (1996) Microglial cells invade the outer retina as photoreceptors degenerate in Royal College of surgeons rats. *Investigative Ophthalmology & Visual Science*, 37(1), 196–203.

Runkle, E.A. & Antonetti, D.A. (2011) The blood-retinal barrier: structure and functional significance. *Methods in Molecular Biology*, 686, 133–148.

Saint-Geniez, M., Kurihara, T., Sekiyama, E., Maldonado, A.E. & D'Amore, P.A. (2009) An essential role for RPE-derived soluble VEGF in the maintenance of the choriocapillaris. *Proceedings of the National Academy of Sciences of the United States of America*, 106(44), 18751–18756.

Silverman, S.M. & Wong, W.T. (2018) Microglia in the retina: roles in development, maturity, and disease. *Annual Review of Vision Science*, 4, 45–77.

Simó, R., Villarroel, M., Corraliza, L., Hernández, C., and Garcia-Ramírez, M.. 2010. The retinal pigment epithelium: something more than a constituent of the blood-retinal barrier—implications for the pathogenesis of diabetic retinopathy. *Journal of Biomedicine & Biotechnology* 2010. 1–15. https://doi.org/10.1155/2010/190724.

Sinha, T., Naash, M.I. & Al-Ubaidi, M.R. (2020) The symbiotic relationship between the neural retina and retinal pigment epithelium is supported by utilizing differential metabolic pathways. *iScience*, 23(4), 101004.

Sparrow, J.R., Hicks, D. & Hamel, C.P. (2010) The retinal pigment epithelium in health and disease. *Current Molecular Medicine*, 10(9), 802–823.

Stefanov, A., Novelli, E., and Strettoi, E.. 2020. Inner retinal preservation in the photoinducible I307N rhodopsin mutant mouse, a model of autosomal dominant retinitis pigmentosa. *Journal of Comparative Neurology*, 528(9), 1502–1522.

Strauss, O. (2005) The retinal pigment epithelium in visual function. *Physiological Reviews*, 85(3), 845–881.

Taylor, A.W., Hsu, S. & Ng, T.F. (2021) The role of retinal pigment epithelial cells in regulation of macrophages/microglial cells in retinal immunobiology. *Frontiers in Immunology*, 12, 724601.

Taylor, A.W., and Ng, T.F.. 2018. Negative regulators that mediate ocular immune privilege. *Journal of Leukocyte Biology*, 10, 1002.

Thanos, S., Pavlidis, C., Mey, J. & Thiel, H.J. (1992) Specific transcellular staining of microglia in the adult rat after traumatic degeneration of carbocyanine-filled retinal ganglion cells. *Experimental Eye Research*, 55(1), 101–117.

Viegas, F.O. & Neuhauss, S.C.F. (2021) A Metabolic Landscape for Maintaining Retina Integrity and Function. *Frontiers in Molecular Neuroscience*, 14, 656000.

Wu, D.M., Ji, X., Ivanchenko, M.V., Chung, M., Piper, M., Rana, P. et al. (2021) Nrf2 overexpression rescues the RPE in mouse models of retinitis pigmentosa. *JCI Insight*, 6(2), e145029. https://doi.org/10.1172/jci.insight.145029

Yang, S., Zhou, J. & Li, D. (2021) Functions and diseases of the retinal pigment epithelium. *Frontiers in Pharmacology*, 12, 727870.

Yu, C., Roubeix, C., Sennlaub, F. & Saban, D.R. (2020) Microglia versus monocytes: distinct roles in degenerative diseases of the retina. *Trends in Neurosciences*, 43(6), 433–449.

Zhang, X., Girardot, P.E., Sellers, J.T., Li, Y., Wang, J., Chrenek, M.A. et al. (2019) Wheel running exercise protects against retinal degeneration in the I307N rhodopsin mouse model of inducible autosomal dominant retinitis pigmentosa. *Molecular Vision*, 25, 462–476.

Zhao, C., Yasumura, D., Li, X., Matthes, M., Lloyd, M., Nielsen, G. et al. (2011) mTOR-mediated dedifferentiation of the retinal pigment epithelium initiates photoreceptor degeneration in mice. *The Journal of Clinical Investigation*, 121(1), 369–383.

Zhou, J., He, S., Zhang, N., Spee, C., Zhou, P., Ryan, S.J. et al. (2010) Neutrophils compromise retinal pigment epithelial barrier integrity. *Journal of Biomedicine & Biotechnology*, 2010, 289360.

Zhou, M., Geathers, J.S., Grillo, S.L., Weber, S.R., Wang, W., Zhao, Y. et al. (2020) Role of epithelial-mesenchymal transition in retinal pigment epithelium dysfunction. *Frontiers in Cell and Developmental Biology*, 8, 501.

How to cite this article: Napoli, D. & Strettoi, E. (2023) Structural abnormalities of retinal pigment epithelial cells in a light-inducible, rhodopsin mutant mouse. *Journal of Anatomy*, 243, 223–234. Available from: https://doi.org/10.1111/joa.13667